

Polarization Diversity for the National Weather Service (NWS), WSR-88D radars

Dusan S. Zrnica
National Severe Storm Laboratory
Norman, OK 73069, USA

In the early eighties the NOAA's National Severe Storms Laboratory (NSSL part of National Ocean and Atmospheric Administration) initiated a study to determine utility of polarization diversity for weather observations. This study culminated with completion of the Joint POLarization Experiment (JPOLE) which unequivocally demonstrated great potential of polarimetric diversity radar.

Common polarization bases are linear and circular. Because most hydrometeors are horizontally oriented the largest contrast in polarization measurements occurs between horizontal and vertical backscattered electric fields. Therefore, and for other practical reasons the chosen scheme employs simultaneous transmission and reception of horizontally and vertically polarized waves. With this scheme all current data acquisition modes and scanning strategies on the WSR-88D (Weather Surveillance Radar-1988 Doppler) remain as is, and the impact of polarimetric implementation on the existing algorithms and products is minimal. The National Weather Service in the US intends to implement this scheme for polarimetric measurements at the end of this decade.

Intense analysis of the outcome of JPOLE experiment proved that polarimetry can address a variety of problems in operational meteorology, like:

- C Improve quantitative precipitation estimation
- C Discriminate hail from rain, possibly gauge hail size
- C Identify precipitation type in winter storms
- C Measure precipitation in the presence of ground clutter
- C Identify electrically active storms
- C Identify presence of insects, birds, and chaff
- C Improve the accuracy of VAD winds
- C Provide initial conditions and constraints to numerical models
- C Identify aircraft icing conditions

Tested were the following polarimetric rainfall estimators:

$$R(Z) = 1.70 \cdot 10^{-2} Z^{0.714} \quad (Z = 300 R^{1.4})$$

$$R(K_{DP}) = 44.0 |K_{DP}|^{0.822} \text{sign}(K_{DP})$$

$$R(Z, Z_{DR}) = 1.42 \cdot 10^{-2} Z^{0.770} Z_{dr}^{-1.67}$$

$$R(K_{DP}, Z_{DR}) = 136 |K_{DP}|^{0.968} Z_{dr}^{-2.86}$$

where

$$[R] = \text{mm} / \text{h} \quad [Z] = \text{mm}^6 \text{m}^{-3} \quad [K_{DP}] = \text{deg} / \text{km} \quad Z_{dr} = 10^{0.1 Z_{DR}(\text{dB})}$$

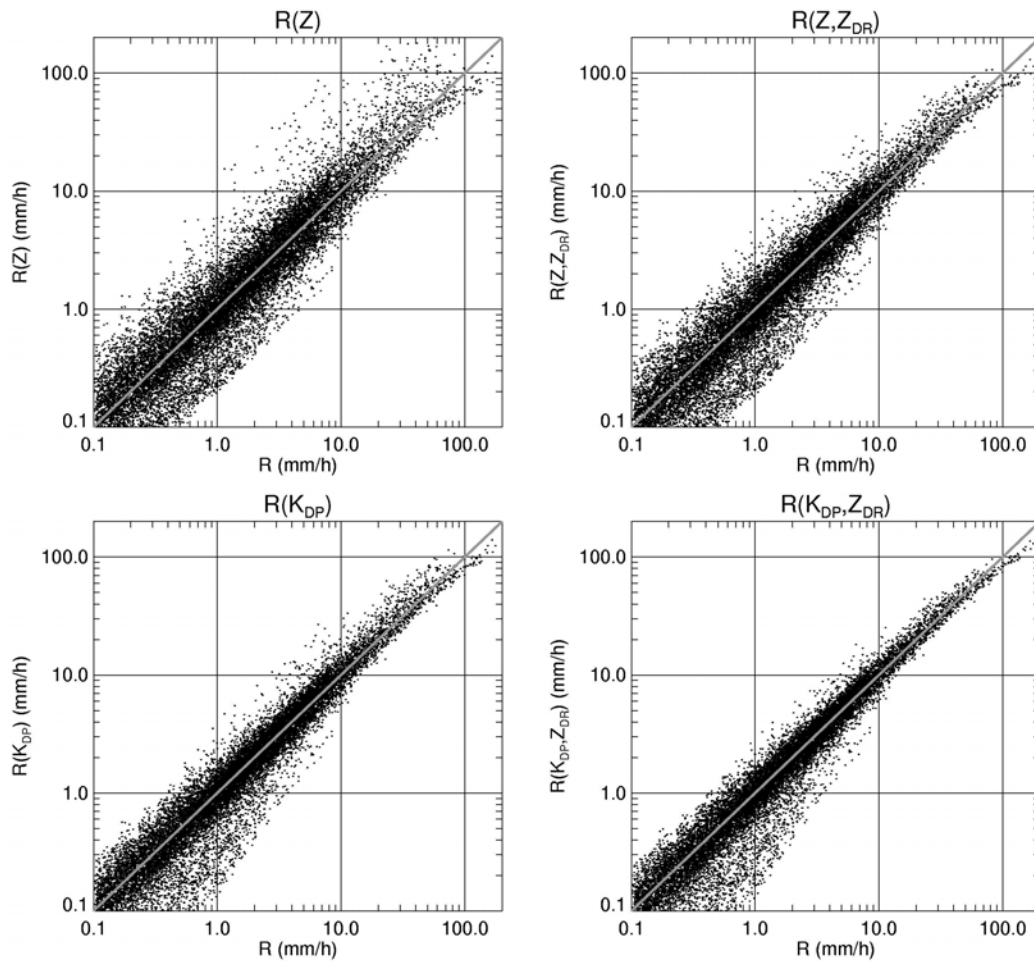


Fig. 1 Sensitivity of different rainfall estimators. Both the actual rain and polarimetric estimates were computed from disdrometer measurements.

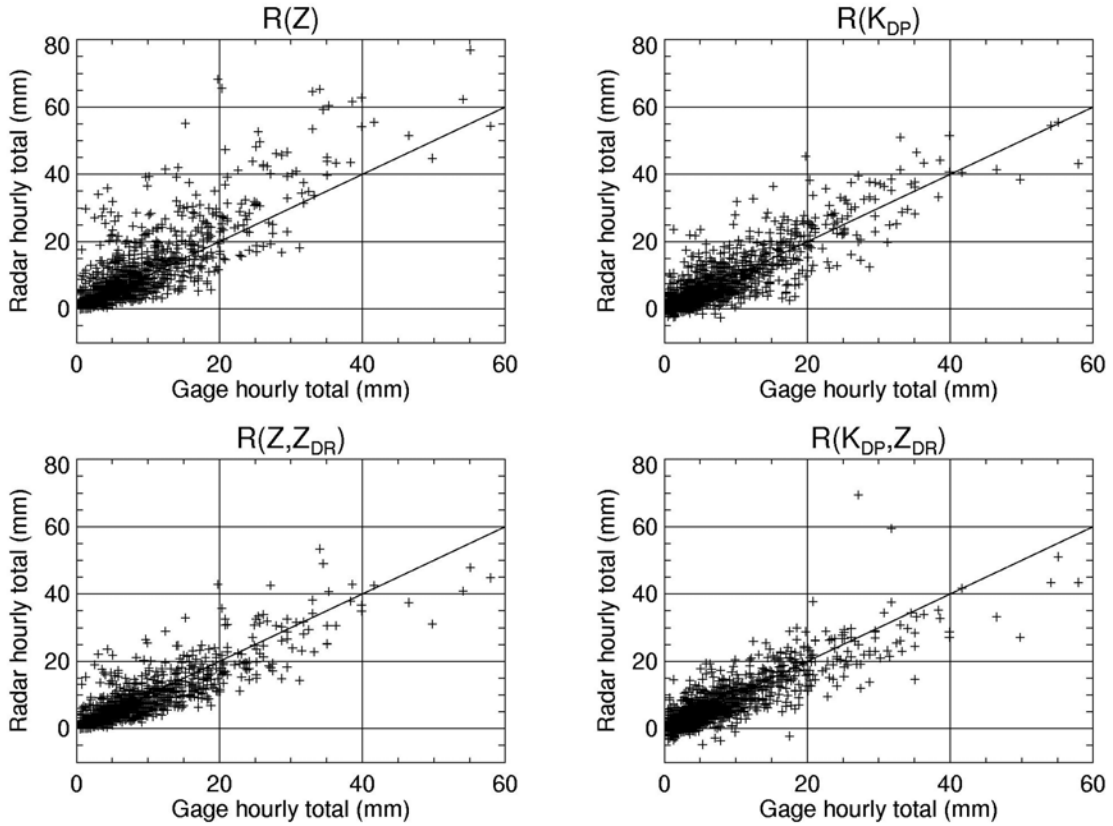


Fig. 2 Sensitivity of different rainfall estimators. The actual rain total is from gages and polarimetric estimates were measured with the radar at 40 to 90 km from the gages (Fig. 3).

Further the following synthetic rainfall estimator was also evaluated:

$$R = R(Z) / f_1(Z_{DR}) \quad \text{if } R(Z) < 6 \text{ mm} / h$$

$$R = R(K_{DP}) / f_2(Z_{DR}) \quad \text{if } 6 < R(Z) < 50 \text{ mm} / h$$

$$R = R(K_{DP}) \quad \text{if } R(Z) > 50 \text{ mm} / h$$

with

$$R(Z) = 1.7010^{-2} Z^{0.714}$$

$$f_1(Z_{DR}) = 0.4 + 5.0 |Z_{dr} - 1|^{1.3}$$

$$R(K_{DP}) = 44.0 |K_{DP}|^{0.822} \text{sign}(K_{DP})$$

$$f_2(Z_{DR}) = 0.4 + 3.5 |Z_{dr} - 1|^{1.7}$$

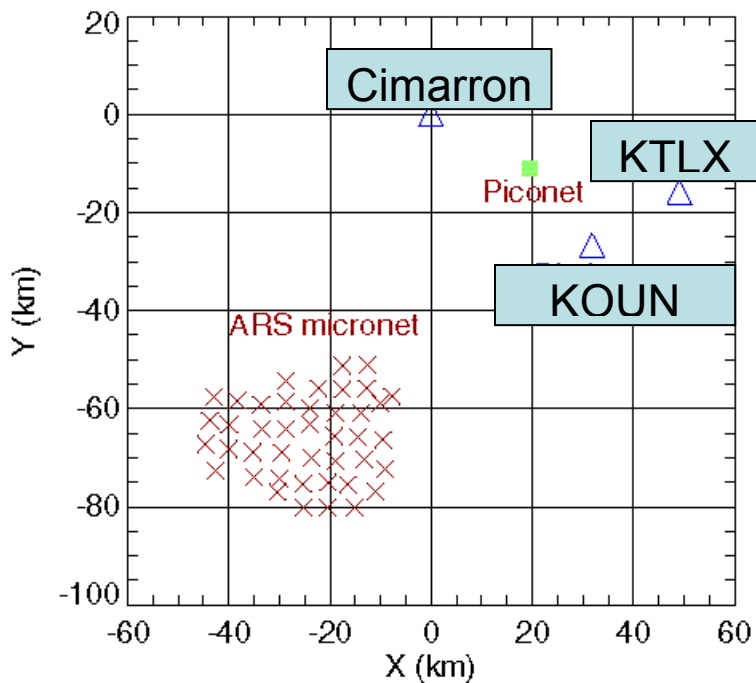


Fig. 3 Location of gages (ARS) and polarimetric radar KOUN.

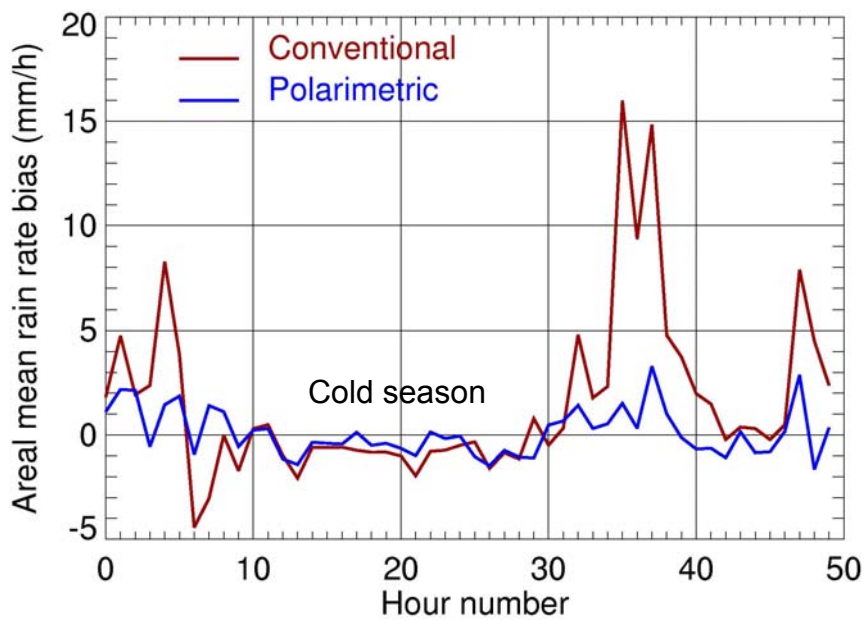


Fig. 4 Mean bias for conventional R(Z) and synthetic polarimetric measurements. Hourly accumulations are from events over two years.

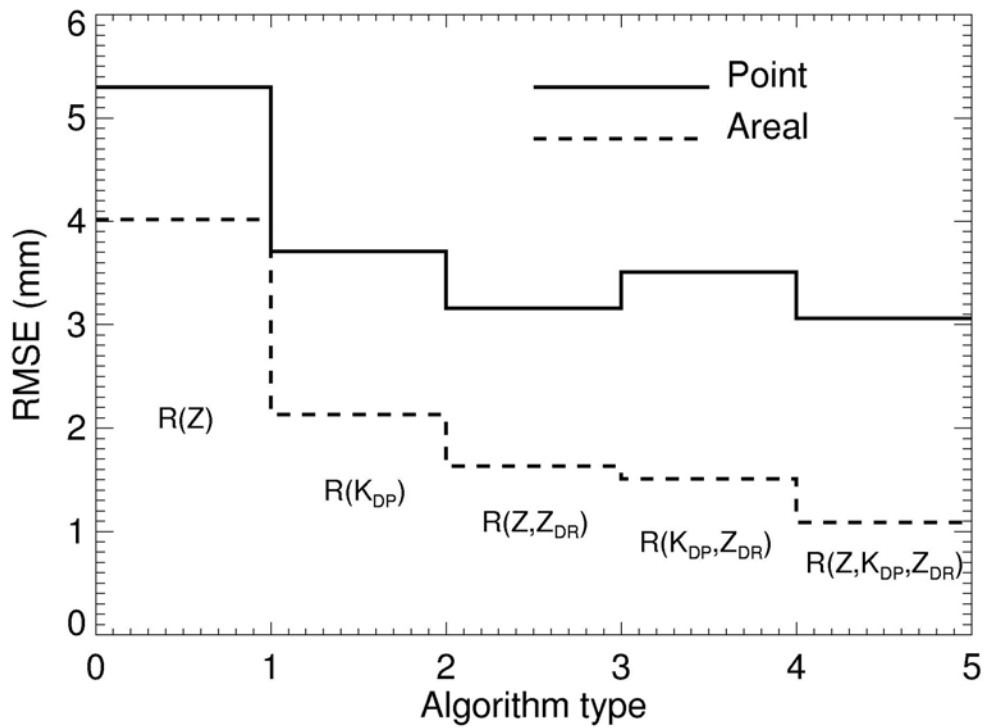


Fig. 5 RMS difference between gages and radar estimates of rain accumulations for areal and point comparison.

Rain Measurement in the Bright Band with $R(Z)$ and $R(K_{DP})$

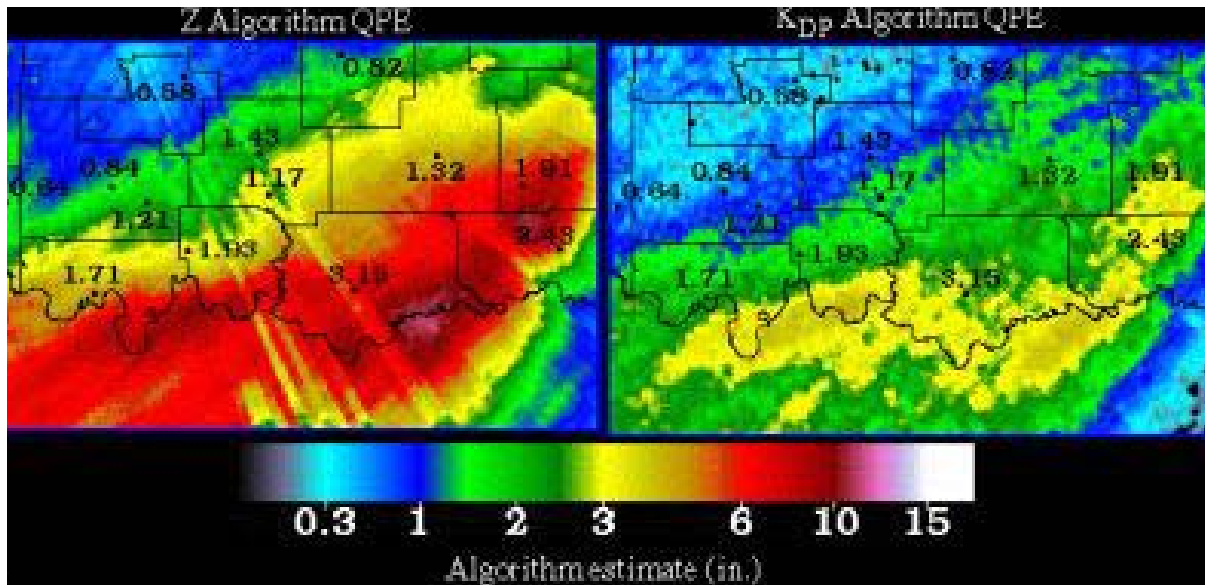


Fig. 6 Two day accumulation of rain (Oct 2002); gage estimates are superposed.

Classification of Hydrometeors

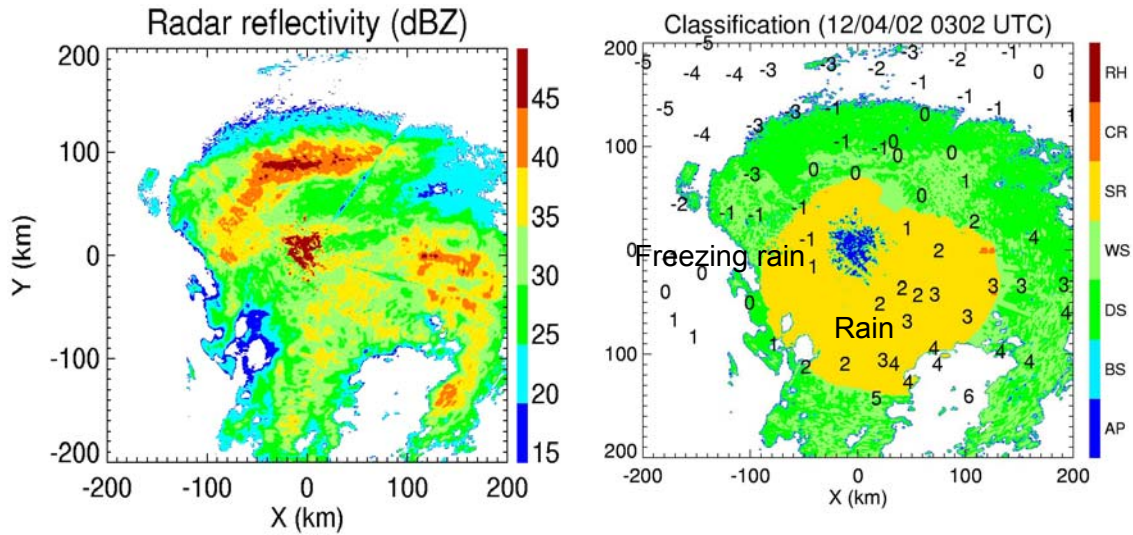


Fig. 7 Discrimination between rain, freezing rain, and snow. Temperature on the ground is superposed.

Transition between rain and snow can be detected, but for identifying freezing rain temperature on the ground is needed.

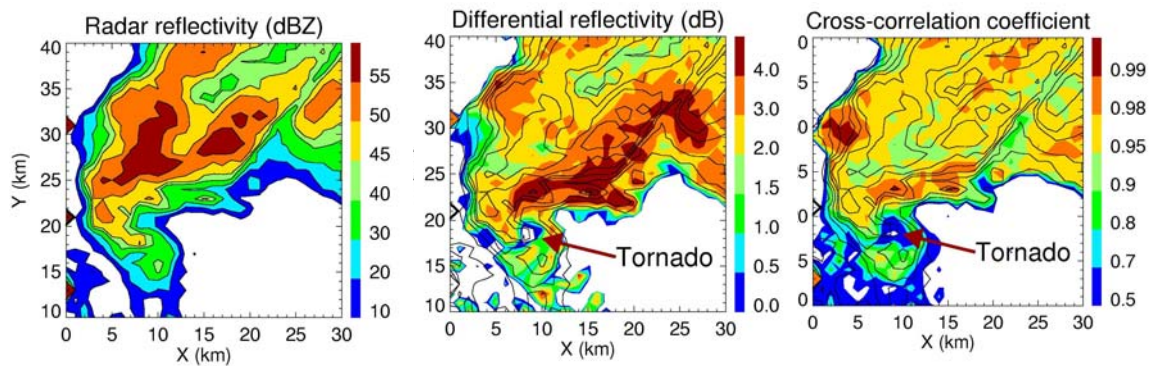


Fig.8 Tornado identification in the fields of differential reflectivity and cross-correlation coefficient.

Once tornado is on the ground it lofts debris which can be detected. Therefore polarimetric signature can confirm tornado on the ground; it can also confirm tornado demise. But it offers no lead time.

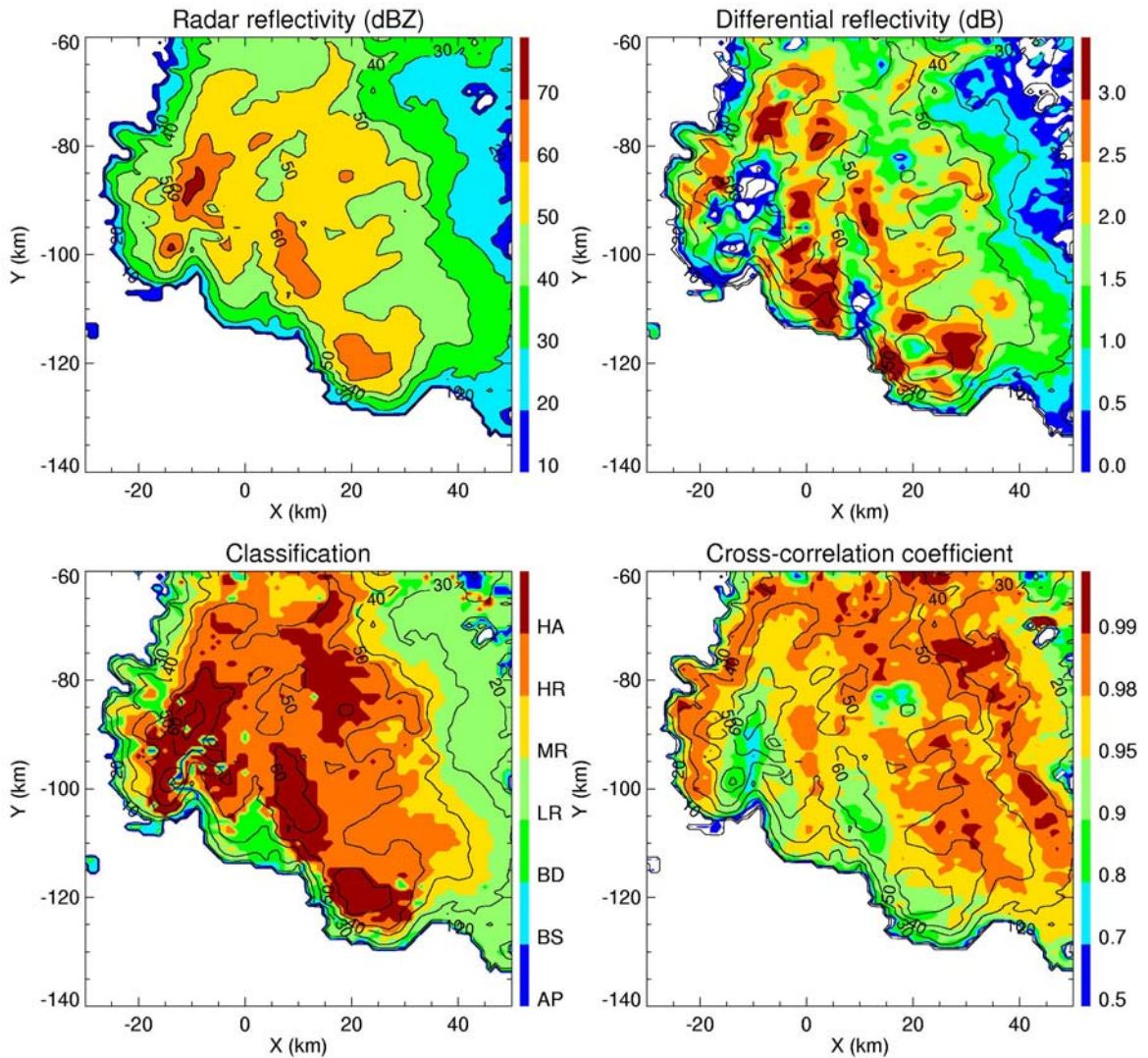


Fig. 9 Detection of Hail. Reflectivity, differential reflectivity and cross correlation fields in a hail storm. HA=hail and rain, HR=heavy rain, MR=moderate rain, LR=light rain, BD=rain with large drops, BS=biological scatterers, and AP=ground clutter (ordinary of seen via anomalous propagation).

Hail detection is direct, based on the values of differential reflectivity (small) and reflectivity (large).

Hail Detection Statistics

Polarimetric method	Conventional method
POD = 88%; FAR=39%; CSI=0.56	POD=100%; FAR=11%; CSI=0.89

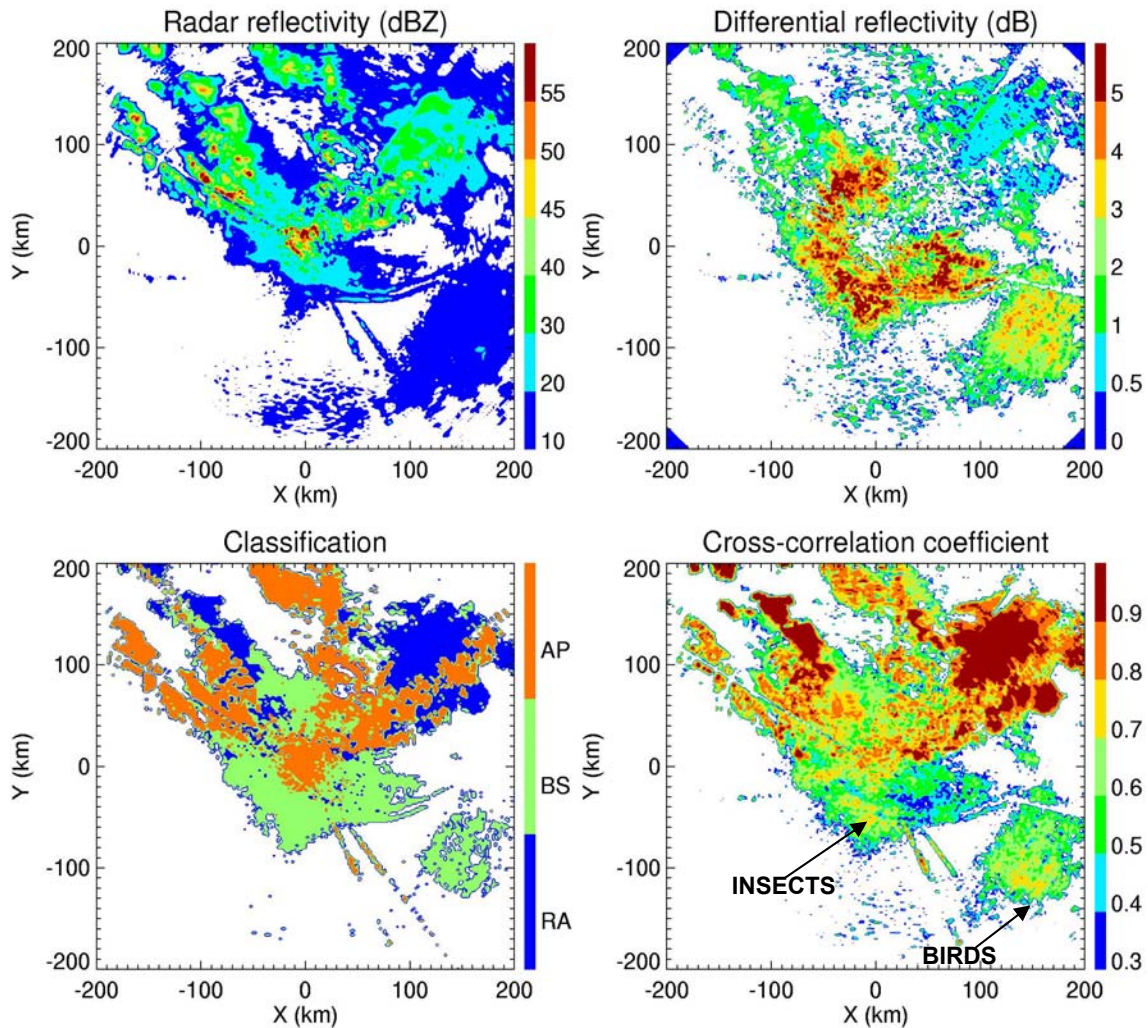


Fig. 10 Discrimination between rain (RA blue), biological scatterers (insects and birds BS green) and ground clutter (including returns via anomalous propagation AP orange).

Several significant improvements in quantitative measurements, data quality, and classification of hydrometeors have been proven, this lead to a decision for polarimetric upgrade of the network. Other less obvious improvements are under investigation.